

#### **OPEN ACCESS**

EDITED BY Brian J. Ferguson, University of Cambridge, United Kingdom

Yoon-Chul Kye, Brigham and Women's Hospital and Harvard Medical School, United States Hongxiang Sun,

Shanghai Jiao Tong University, China

\*CORRESPONDENCE

Ewart W. Kuijk

☑ e.w.kuijk-3@umcutrecht.nl
Edward E. S. Nieuwenhuis

≥ e.nieuwenhuis@prinsesmaximacentrum.nl

#### <sup>†</sup>PRESENT ADDRESS

Pharma,

Research and Early Development, F. Hoffmann-La Roche Ltd, Basel, Switzerland

<sup>‡</sup>These authors have contributed equally to this work and share last authorship

RECEIVED 01 August 2025 ACCEPTED 29 September 2025 PUBLISHED 15 October 2025

### CITATION

De Vries MH, Meddens CA, Hijma HJ, Berrens A-C, Jansen SA, Kooiman BAP, Snapper S, Clevers H, Mokry M, Kuijk EW and Nieuwenhuis EES (2025) Human colon stem cells are the predominant epithelial responders to bacterial antigens. Front. Immunol. 16:1677943. doi: 10.3389/fimmu.2025.1677943

### COPYRIGHT

© 2025 De Vries, Meddens, Hijma, Berrens, Jansen, Kooiman, Snapper, Clevers, Mokry, Kuijk and Nieuwenhuis. This is an open-access article distributed under the terms of the Creative Commons Attribution License (CC BY).

The use, distribution or reproduction in other forums is permitted, provided the original author(s) and the copyright owner(s) are credited and that the original publication in this journal is cited, in accordance with accepted academic practice. No use, distribution or reproduction is permitted which does not comply with these terms.

# Human colon stem cells are the predominant epithelial responders to bacterial antigens

Maaike H. De Vries<sup>1,2</sup>, Claartje A. Meddens<sup>1,2</sup>, Hemme J. Hijma<sup>1,2</sup>, Anne-Claire Berrens<sup>1,2</sup>, Suze A. Jansen<sup>1,2</sup>, Berend A. P. Kooiman<sup>1,2</sup>, Scott Snapper<sup>3</sup>, Hans Clevers<sup>4,5,6†</sup>, Michal Mokry<sup>1,2,7,8</sup>, Ewart W. Kuijk<sup>1,2,9\*‡</sup> and Edward E. S. Nieuwenhuis<sup>6,10\*‡</sup>

<sup>1</sup>Department of Pediatric Gastroenterology, Wilhelmina Children's Hospital, University Medical Center Utrecht, Utrecht, Netherlands, <sup>2</sup>Regenerative Medicine Center Utrecht, University Medical Center Utrecht, Utrecht, Netherlands, <sup>3</sup>Division of Gastroenterology, Hepatology and Nutrition, Department of Pediatrics, Boston Children's Hospital, Boston, MA, United States, <sup>4</sup>Oncode Institute, Princess Máxima Center for Pediatric Oncology, Utrecht, Netherlands, <sup>5</sup>Hubrecht Institute, Royal Netherlands Academy of Arts and Sciences and University Medical Center Utrecht, Utrecht, Netherlands, <sup>6</sup>Princess Máxima Center for Pediatric Oncology, Utrecht, Netherlands, <sup>7</sup>Laboratory of Experimental Cardiology, University Medical Center Utrecht, Utrecht, Netherlands, <sup>8</sup>Laboratory of Clinical Chemistry and Hematology, Division Laboratories and Pharmacy, University Medical Center Utrecht, Utrecht, Netherlands, <sup>9</sup>Lab of Cellular Disease Models, Department of Pediatrics, Regenerative Medicine Center Utrecht, University Medical Center Utrecht, Utrecht, Netherlands, <sup>10</sup>Wilhelmina Children's Hospital, University Medical Center Utrecht, Utrecht, Netherlands

Intestinal epithelial cells (IECs) are capable of mounting an adequate antimicrobial inflammatory response to pathogens while tolerating commensals. The underlying regulatory mechanisms of immune sensitivity remain incompletely understood, particularly in the context of human IECs. To enhance our understanding of the immune response of IECs to bacterial epithelial barrier breach, we investigated whether epithelial responsiveness is contingent on cell identity and cell polarization. We exposed human intestinal organoids to bacterial antigens to study their immune responses. Notable discrepancies were observed in the specific reactions exhibited by intestinal stem cells (ISCs) and enterocytes. It was determined that basolateral exposure of IECs to bacterial antigens resulted in a robust response, whereas apical exposure elicited a significantly more modest response. We identified ISCs as the principal responders, while the reaction of enterocytes was found to be attenuated. The regulation of bacterial responsiveness in enterocytes occurs at multiple levels, including the modulation of NFkB activation and post-transcriptional control of mRNA stability. Our findings demonstrate that differentiated non-responsive enterocytes can be sensitized to bacterial antigens through the activation of

the WNT pathway. These findings extend the crucial role of WNT signaling for intestinal epithelial homeostasis and regulation of stem cell maintenance, proliferation, differentiation, and tissue architecture in the gut. Additionally, they reveal a new function of WNT signaling in regulating microbial responses within the intestinal environment.

KEYWORDS

intestinal stem cells, intestinal epithelium, innate immunity, immune regulation, WNT pathway, inflammatory bowel disease

### 1 Introduction

The large intestine is populated by a vast number of commensal microorganisms, resulting in a constant microbial exposure of the intestinal epithelial cells (IECs) (1, 2). Under physiological conditions, IECs do not elicit an inflammatory response (3), however, inflammatory responses are necessary upon encountering pathogenic bacteria or during epithelial barrier disruption to prevent microbial invasion and dissemination into the bloodstream. Failure of IECs to maintain a balance between responsiveness and non-responsiveness during continuous microbial challenge (4, 5) can lead to chronic inflammation as observed in Inflammatory Bowel Disease (IBD).

The responsiveness of cells to microbes is dependent on the presence of Pattern Recognition Receptors (PRRs) and the expression and modification of molecules involved in intracellular signal transduction as well as various transcriptional and post-transcriptional processes (6, 7). PRRs have the capacity to activate a multitude of immune response pathways, including the NFκB pathway (8). In its inactive state, NFκB is bound to an inhibitor, IκB, which keeps it sequestered in the cytoplasm. Upon activation, IκB is phosphorylated and subsequently degraded, thereby releasing NFκB and enabling its entry into the nucleus. Within the nucleus, NFκB binds to specific DNA sequences in the promoter regions of target genes, thereby promoting transcription of NFκB target genes, including CXCL8, TNFalpha, and NFKBIA (8, 9). The innate immune response requires minutes to hours to be fully activated upon stimulation (10).

PRRs are differentially expressed in the different epithelial cell types and along the apical basolateral axis, which may cause cell type specific responses (11–13). All epithelial cell types originate from intestinal stem cells (ISCs) that reside at the bottom of the crypts. Differentiated progeny that emerge from these stem cells migrate towards the top of the villi of the small intestine or the inter-crypt regions of the colon, where the cells are shed into the lumen (14). The self-renewal, proliferation and differentiation of ISCs are largely regulated by the WNT signaling pathway, which

**Abbreviations:** ARE, AU-rich element; ChIP, chromatin immuno-precipitation; IBD, Inflammatory bowel disease; IECs, Intestinal epithelial cells; ISCs, Intestinal stem cells; PRR, Pattern recognition receptors; qPCR, quantitative polymerase chain reaction; TLRs, Toll like receptors; 3'UTR, 3'untranslated region.

exhibits differential activity along the crypt-differentiation axis, with the highest activity observed in the crypt (15).

The precise relationship between differentiation state, responsiveness, and bacterial signaling remains unclear, as does the impact of bacterial signaling on cell identity (16-18). While innate immunity pathways have been extensively studied in myeloid-derived cell types (19, 20), there is increasing interest for the role of for these pathways in IECs with most studies conducted in mouse models and immortalized cell lines. While these model systems provide valuable insights, each model has inherent limitations in studying immune responsiveness (21-23), such as intrinsic discrepancies between human and murine immune responses (21-25) and genetic aberrations that influence the responsiveness of human immortalized cell lines. Moreover, cell lines represent only a single cell type with incomplete cell differentiation and lack variation in genetic background (21-23, 26). Human intestinal organoids can overcome these limitations, as they are derived from human ISCs isolated from epithelial biopsies and can be differentiated into various IEC types (27, 28). Therefore, human intestinal organoids can be used to study the microbe interaction in an isolated setting (29-31).

The objective of this study is to investigate the immune responses in ISCs and differentiated IECs using human intestinal organoids exposed to *E. Coli* antigens. Our findings reveal disparities in immune responsiveness to bacterial antigens between ISCs and enterocytes, the most prevalent differentiated cell type of the intestinal epithelium. This study further explores the molecular mechanisms that underlies high responsiveness of ISCs and low responsiveness of enterocytes, dissecting the involved immune pathways at multiple levels, ranging from NFκB activation to post-transcriptional regulation of inflammatory gene transcripts. Our findings indicate that the intestinal immune response is, regulated processes upstream as well as downstream of NFκB activation with a governing role for the WNT pathway.

### 2 Materials and methods

### 2.1 Medical and ethical guidelines

Biopsies were obtained via ileo-colonoscopies and gastroscopies, which were conducted as part of the standard diagnostic procedure.

Data collection and research studies were conducted in adherence to the ethical guidelines established by the ethics committees. Human Material Approval for this study was obtained from the Ethics Committees University Medical Center Utrecht (Medisch Ethische Toetsings Commissie (METC) protocol #10/402, titled: Specific Tissue Engineering in Medicine (STEM)) or Boston Children Hospital (protocol #IRB-P00000529, titled: Pediatric Gastrointestinal Disease Biospecimen Repository and Data Registry).

### 2.2 Organoid culturing

Biopsies of the uninflamed colon and ileum were obtained from patients via colonoscopy for gastrointestinal symptoms indicative of IBD or CRC, but for who both IBD and CRC were ultimately ruled out as the underlying condition based on pathological assessment. The biopsies exhibited no macroscopic or pathological abnormalities. Crypt isolation and culture of human intestinal cells from biopsies were performed in accordance with the previously described methodology (28, 32). The organoids were maintained long-term in a stem cell medium, which consisted of in Advanced medium/F12 (Gibco, 12634028) containing RSPO1, noggin, EGF (Peprotech, 315-09-1MG), A83-01 (Tocris Bioscience, 2939/10), nicotinamide (SIGMA-ALDRICH, N0636-500G), SB202190 (SIGMA-ALDRICH, S7067-25mg), and WNT3A. To induce differentiation, the cultures were maintained for 5-7 days in enterocyte medium, which is stem cell medium lacking nicotinamide, SB202190, and WNT3A. The conditioned media for RSPO1 (stably transfected RSPO1 HEK293T cells were kindly provided by Dr. C. J. Kuo, Department of Medicine, Stanford, CA), noggin, and WNT3A were utilized. The medium was refreshed every 2-3 days and the organoids were passaged at a ratio of 1:4 approximately every 10 days (detailed media composition: Supplementary Table S1.

Matrigel-embedded organoids (3D) were cultured in 70% Matrigel (BD Biosciences), diluted using growth factor-deficient medium (GF-), which consisted of Advanced DMEM supplemented with penicillin/ streptomycin (GIBCO, 15140122), 1M HEPES (GIBCO, 15630080) and Glutamax 100x (GIBCO, 35050061). The primary intestinal organoids were cultured at 37°C, in 5% CO2. Intestinal epithelial monolayers (2D) were prepared according to the methodology previously described (33). In brief, transwells (Corning Costar, Tewksbury, MA, USA) were coated with Matrigel (1:40 in PBS+ with Ca/Mg, Sigma-Aldrich, D8662-500ML) for 1 hour at RT. Subsequently, 2.5\*10<sup>5</sup> single cells were seeded on a transwell insert in the corresponding 24-well plate. A volume of 100µL and 600µL of medium was utilized in the apical and basolateral compartments, respectively. The monolayers were cultivated until they reached confluence, which was determent through microscopy and transepithelial electrical resistance (TEER) measurement. The primary intestinal monolayers were cultured at 37 °C, in 5% CO2 environment.

### 2.3 Exposure to bacterial antigens

A bacterial lysate was prepared from E. coli HST-08 Stellar competent cells (Takara Bio, 636766). The bacteria were subjected

to a 20-min heat-inactivated process at 75 °C, pooled in sterile PBS, and subsequently frozen for 1h at -80 °C. Subsequently, the samples were subjected to sonicated using a Covaris ultrasonicator with the following settings: duty cycle of 20%; intensity of 10; cycles per burst of 500, and a total sonication time of 30 sec in a 13x65mm glass vial (Covaris), subjected to centrifugation at 10,000g for 30 min at 4 °C, and subsequently filtered through a sterilizing filter. The quantity of bacterial lysate utilized for organoid exposure was determined through a titration process, ranging from 1µL to 20µL of lysate per 500µL medium. This was done to ascertain the concentration that elicits half of the maximum CXCL8 response on mRNA in 3D cultures. Stem cell-enriched organoids were exposed at day 7-10, and enterocyte-enriched organoids were exposed after 5 days of differentiation. The same bacterial lysate concentrations were employed in 3D, and 2D apical and basolateral exposure experiments. In experiments involving multiple days of exposure, a new bacterial lysate was added at each medium refreshment (approx. every 2 days).

### 2.4 RNA isolation and qPCR

RNA was isolated with TRIzol<sup>®</sup> LS (Ambion, cat. no. 10296-028), in accordance with the manufacturer's protocol. cDNA was synthesized through reverse transcription (Invitrogen, Carlsbad, CA or iScript, Biorad, Hercules, CA, 1708891). Messenger RNA (mRNA) abundances were determined by real-time PCR using validated primer pairs and SYBR Green (Bio-Rad, Hercules, CA, 1708886). ACTB mRNA abundance was employed for normalization purposes. The following qPCR primers were utilized: *LGR5* forward GAATCCCCTGCCCAGTCTC, *LGR5* reverse ATTGAAGGCTTCGCAAATTCT, β-actin forward TGG CACCCAGCACAATGAA, β-actin reverse CTAAGTCATAGTCC GCCTAGAAGCA, NFKBIA forward GCAAAATCCTGACCTGG TGT, NFKBIA reverse GCTCGTCCTCTGTGAACTCC, CXCL8 forward GGCACAAACTTTCAGAGACAG, CXCL8 reverse ACACAGAGCTGCAGAAATCAG.

### 2.5 Luminex

At the time of harvesting, the medium from organoids was collected (after 6h exposure) and was stored at -80 °C. The concentrations of IL8, IL23, MIP3a, GRO1a, LIF, MCP1, TNFa, ENA78, and GCP2 were measured using the Luminex technology as previously described (34).

### 2.6 RNA sequencing

RNA was isolated with TRIzol<sup>®</sup> LS (Ambion, cat. no. 10296-028), in accordance with the manufacturer's protocol. Libraries were generated using NEXTflexTM Rapid RNA-seq Kit (Bio Scientific) and sequenced by the Nextseq500 platform (Illumina) to produce 75 bp single-end reads at the Utrecht DNA sequencing

facility. Reads were aligned to the human reference genome GRCh37 using STAR. Differentially expressed genes in the transcriptome data were identified using the DESeq2 package with standard settings (35). RPM values were calculated using edgeR's RPKM function.

### 2.7 Explants

Colon biopsies were washed and cultured in stem cell medium (described above) for 24h. Thereafter, the explants were stimulated with bacterial lysate for 6h. Next, RNA was then isolated and sequenced as described above.

### 2.8 Pathway analysis, functional enrichment, GSEA, and KEGG pathway analysis

Functional enrichment was performed with the R-package clusterProfiler (36–38), while GSEA was carried out with the packages gage and gageData were used (39). KEGG pathway analysis was performed using the KEGG pathway analysis package (40).

### 2.9 Immunohistochemistry

The organoids were collected by meticulous disruption of the Matrigel and sequential elimination of the Matrigel through centrifugation (5 min, 2000rpm). The samples were subsequently fixed in 4% formaldehyde and embedded in 200 $\mu$ L of 2% agarose in dH2O, prior to embedding the samples in paraffin. Slides with a thickness of 5 $\mu$ m were deparaffinized and subjected to heatmediated antigen retrieval was performed for a period of 20 min in a citrate antigen retrieval buffer with a pH of 6 (Sigma-Aldrich, C9999). The slides were blocked for 30 min in 5% BSA at RT and incubated ON at 4 °C with primary antibodies (mouse  $\alpha$ -NF $\kappa$ B p65 L8F6 1:50 (CST 6956S, Cell signaling Technology) in 5% BSA-PBS). Subsequently, the slides were incubated with secondary antibodies Alexa 488 donkey-anti-mouse (1:400 (A21202, Thermo Fisher Scientific)) for 1h a RT. Images were captured with a 63x objective on a Leica TCS SP8 X confocal microscope.

### 2.10 NFkB-inhibition

Duodenum organoids were cultivated from single cells on stem cell medium. 8 Days after seeding, the organoids were treated with NFkB-inhibitors:  $5\mu M$  IMD 0354 (Abcam, ab144823) or  $10\mu M$  TPCA 1 (Abcam, ab145522). Following the addition of the inhibitors after12h of inhibitors, the organoids were exposed to bacterial lysate for 6h, after which RNA was isolated.

### 2.11 CHIR99021

Intestinal organoids generated from single cells using stem cell medium. The organoids were cultured from single cells for 10–14 days, either on stem cell medium or by differentiating them into enterocytes for the 5 days on enterocyte medium. 3mM of CHIR99021 (Bio-Techne, 4423/10) (14, 41) were added 18h prior to exposure of bacterial lysate for 6h, after which RNA was isolated.

### 2.12 Single-cell RNA sequencing

Colon and ileum-derived organoids were cultured for 10-14 days from single cells in 3 conditions: 1) on stem cell medium during the whole experiment, 2) stem cell medium was changed to enterocyte medium for the last 24 hours before harvesting, 3) stem cells medium was changed for the last 4 days before harvesting. For each condition half of the organoids were exposed for 6h with bacterial lysates before harvesting. Subsequently, cells were trypsinized and FACS-sorted using Propidium Iodide (PI) (Thermo Fisher Scientific - P3566) to eliminate dead cells into 384-well pre-indexed plates per condition. The plates were processed by Single Cell Discoveries as described previously using SORT-seq technology (42). The data were analyzed using the Seurat V2.3.4. software package after excluding mitochondrial and ribosomal gene and a set of unreliably mapped genes (UGDH-AS1, PGM2P2, LOC100131257, MALAT1, KCNQ1OT1, PGM5P2, MAB21L3, EEF1A1) with these parameters: CreateSeuratObject(min.cells = 3, min.genes = 1500), NormalizeData(normalization.method = "LogNormalize", scale.factor = 10000), FindVariableGenes (mean.function = ExpMean, dispersion.function = LogVMR, x.low.cutoff = 0.0125, x.high.cutoff = 3, y.cutoff = 0.5), FindClusters (reduction.type = "pca", dims.use = 1:12, resolution = 0.6).

### 2.13 Chromatin immuno-precipitation sequencing

ChIP was conducted using the MAGnify ChIP kit (Invitrogen, Carlsbad, CA) in accordance with the manufacturer's instructions.  $1\mu L$ α-acetylated histone 3 lysine 27 (H3K27ac) (ab4729; Abcam) or 1μL αtrimethylated lysine 4 (H3K4me3) (#39159; Active Motif) was utilized per immunoprecipitation. The captured DNA was purified using the ChIP DNA Clean & Concentrator kit (Zymo Research). The libraries were prepared using the NEXTflex TM Rapid DNA Sequencing Kit (Bioo Scientific). The samples were PCR amplified, checked for the proper size range and for the absence of adaptor dimers on a 2% agarose gel, and barcoded libraries were sequenced 75 bp single-end on Illumina NextSeq500 sequencer. The sequencing reads were mapped against the reference genome (hg19 assembly, NCBI37) using the BWA package (mem -t 7 -c 100 -M -R)42. Multiple reads mapping to the same location and strand were collapsed to single read and used for peak-calling. Peaks/regions were called using Cisgenome 2.043 (-e 150 -maxgap 200 -minlen 200).

### 2.14 ARE-enrichment

ARE-enrichment was calculated using the ARED-plus database (43). The percentage of response genes (genes upregulated upon 6h exposure to bacterial lysate), stem genes (genes upregulated in stem cell medium without exposure, Supplementary Table S2) or differentiation genes (genes upregulated in enterocyte medium without exposure, Supplementary Table S2) that have at least one AU-rich element encoded in the 3'UTR was calculated per gene set.

### 2.15 Poly(A)-assay

Colon organoids were cultured from single cells for a period of 10–14 days, either in stem cell medium or organoids were differentiated for the 5 days on enterocyte medium. All organoids were subjected to bacterial lysate for 6h before RNA isolation, as previously described. GI-tailing and reverse transcription were done using the Poly(A)-tail length assay kit (ThermoFisher Scientific, #764551KT) and according to the manufacturer's protocol. Next, amplification of individual genes was done with a gene specific forward primer (CXCL8 CTTGTCATTGCCAGCTGTGT, GAPDH CAACGAATTTGGCTACAGCA,  $\beta$ -actin ATCCTAAAAGCCA CCCCACT, CXCL1 GGCATACTGCCTTGTTTAATGG, CXCL2 CACAGTGTGTGGTCAACATTTCT, CCL2 GATACAGAGACTTG GGGAAATTG) and a GI-tail reverse primer (Poly(A) tail length assay kit) for 35 cycles in Platinum PCR SuperMix High Fidelity (Invitrogen, #12532016). Samples were analyzed on a 2% agarose gel.

### 3 Results

### 3.1 Epithelial cells mainly respond to bacterial antigens when exposed basolaterally and in a stem cell state.

The intestinal epithelium, in conjunction with the mucosal layer, serves as the primary cellular defense mechanism against the gut microbiota (44, 45). To investigate the responsiveness of IECs to microbial antigens, we utilized healthy, human colon-derived organoids and exposed them to a bacterial lysate. To assess the responsiveness of ISCs versus enterocytes, we conducted a comparative analysis of the effects of bacterial stimulation on undifferentiated stem cell-enriched organoids and differentiated enterocyte-enriched organoids followed by RNA-seq. Like the stem cells of the crypts, stem cell-enriched organoids have high WNTpathway activity, while enterocyte organoids have low WNT-pathway activity. Enterocyte organoids were obtained from stem cell enriched organoids after five days of differentiation in the absence of WNT and successful differentiation was confirmed by analysis of the expression of marker genes in RNA sequencing data (Supplementary Figure S1). Following a six-hour exposure to bacterial lysates, the undifferentiated organoids exhibited a strong response leading to the differential expression of over 1,000 genes (712 upregulated and 314 downregulated; Figure 1A and Supplementary Table S3). This time point was used as a reference in all subsequent assays, unless otherwise indicated. The response is characterized by the upregulation of numerous inflammatory genes, including *TNFalpha*, *CXCL8*, *NFKB2*, and *NFKBIA*. Enterocyte organoids exhibited a weak response to bacterial lysate with less than 100 differentially expressed genes (61 upregulated and 17 downregulated) (Figure 1B; Supplementary Table S4; Supplementary Figure S2A). The baseline expression levels of *CXCL8* demonstrated a comparable expression between unexposed stem cell-enriched organoids and enterocyte-enriched organoids (Figure 1C). This shows that the difference in *CXCL8* expression upon exposure cannot be explained by a higher baseline expression level in undifferentiated cells.

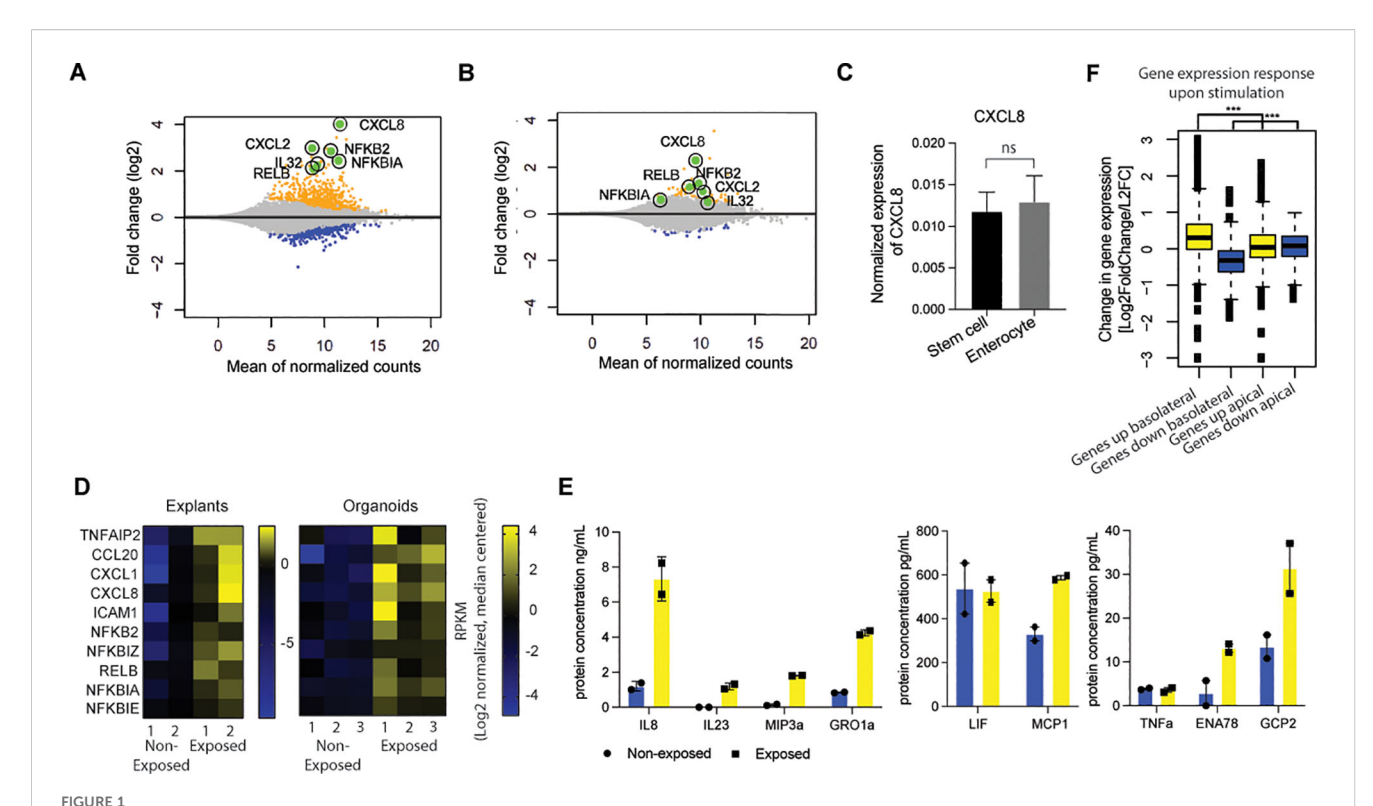
Notably, we conducted a bulk RNA transcriptomics analysis of healthy colon explants (i.e., intact biopsies) and undifferentiated organoids exposed to bacterial lysates. The explants exhibited expression patterns analogous to those identified in the stem cell-enriched organoid model, indicating that the organoid experiments could be representative of responses from a completer tissue sample (Figure 1D). In addition, we show heterogeneity in expression of various cytokine and NFkB-related genes (Figure 1D; Supplementary Figure S2A).

Next, we analyzed the secretion of Interleukin-8 (IL8) protein when exposed to bacterial lysate. The colon stem cell-enriched organoids secreted IL8, IL23, MIP3a, GRO1a, LIF, MCP1, TNFα, ENA78, and GCP2 (encode by genes *CXCL8, IL23, CCL20, CXCL1, LIF, CCL2, TNF, CXCL5, and CXCL6*, respectively) upon exposure (Figure 1E). It can be concluded that the responses observed in the *in vitro* system reflect the intestinal epithelial inflammatory responses.

In physiological conditions, the intestinal epithelium is exposed exclusively to bacteria at the apical (luminal) surface only. To investigate the impact of cell polarity on microbial responsiveness, organoids were cultivated as monolayers that were exposed from the apical or the basolateral side. In contrast to the robust response observed upon basolateral exposure, apical responses were found to be attenuated under similar conditions (Figure 1F; Supplementary Figure S2B). These findings suggest that in the in vivo situation, epithelial cells within the intestinal crypt only respond when the barrier that allows for microbial molecule passage is disrupted, resulting in basolateral exposure. This can occur when the barrier function of the intestinal epithelium is affected due to, for example, invasive microorganisms, genetic defects that are associated with increased epithelial permeability layer (46, 47) or disruption of the epithelium as observed in the inflamed intestinal mucosa of patients with IBD (48, 49). Additionally, an uneven distribution of receptors along the apical-basolateral axis may contribute to the observed differences in apical and basolateral responsiveness (12, 13).

# 3.2 Single cell RNA sequencing shows that intestinal stem cells give a higher inflammatory response compared to enterocytes

To gain further insight into the specific responses of healthy human epithelial cell types during a breach of the epithelial barrier in their various states of differentiation, we performed single cell



Epithelial cells mainly respond to bacterial antigens when exposed basolaterally and in a stem cell state. (A) MA-plot-visualization of the log ratio and mean value of bulk RNAseq from healthy colon-derived stem cell-enriched organoids upon exposure to microbial antigens for 6h. (n=2). (B) MA-plot visualization of the log ratio and mean value of bulk RNAseq from healthy colon-derived enterocyte-enriched organoids upon exposure to microbial antigens for 6h. (n=2). (C) qPCR of CXCL8 of unexposed healthy colon-derived stem cell-enriched organoids and healthy colon-derived enterocyte-enriched organoids. Error bars indicate SEM (unpaired t-test) (n=3). (D) Expression patterns of inflammatory genes of bulk RNAseq in healthy colon-derived stem cell-enriched organoids (exposed/non-exposed) compared to healthy colon explants (exposed/non-exposed). (E) Luminex analysis of Interleukin-8 (IL8), IL23, MIP3a, GRO1a, LIF, MCP1, TNFa, ENA78, and GCP2 release by healthy colon-derived stem cell-enriched organoids upon exposure to bacterial antigens 6h (n=2). Error bars indicate SEM. (F) Expression changes of response genes were measured by bulk RNA-seq healthy colon-derived stem cell-enriched organoids grown as a monolayer and exposed from either the apical or basolateral side for 6h. Average genes up or down regulated. Statistical significance was determined using the Wilcoxon rank-sum test n=2. (results of the statistical test – as noted in the figure legend: ns = p > 0.05; \*p ≤ 0.05; \*\*p ≤ 0.01; \*\*\*p ≤ 0.001) qPCR = quantitative polymerase chain reaction.

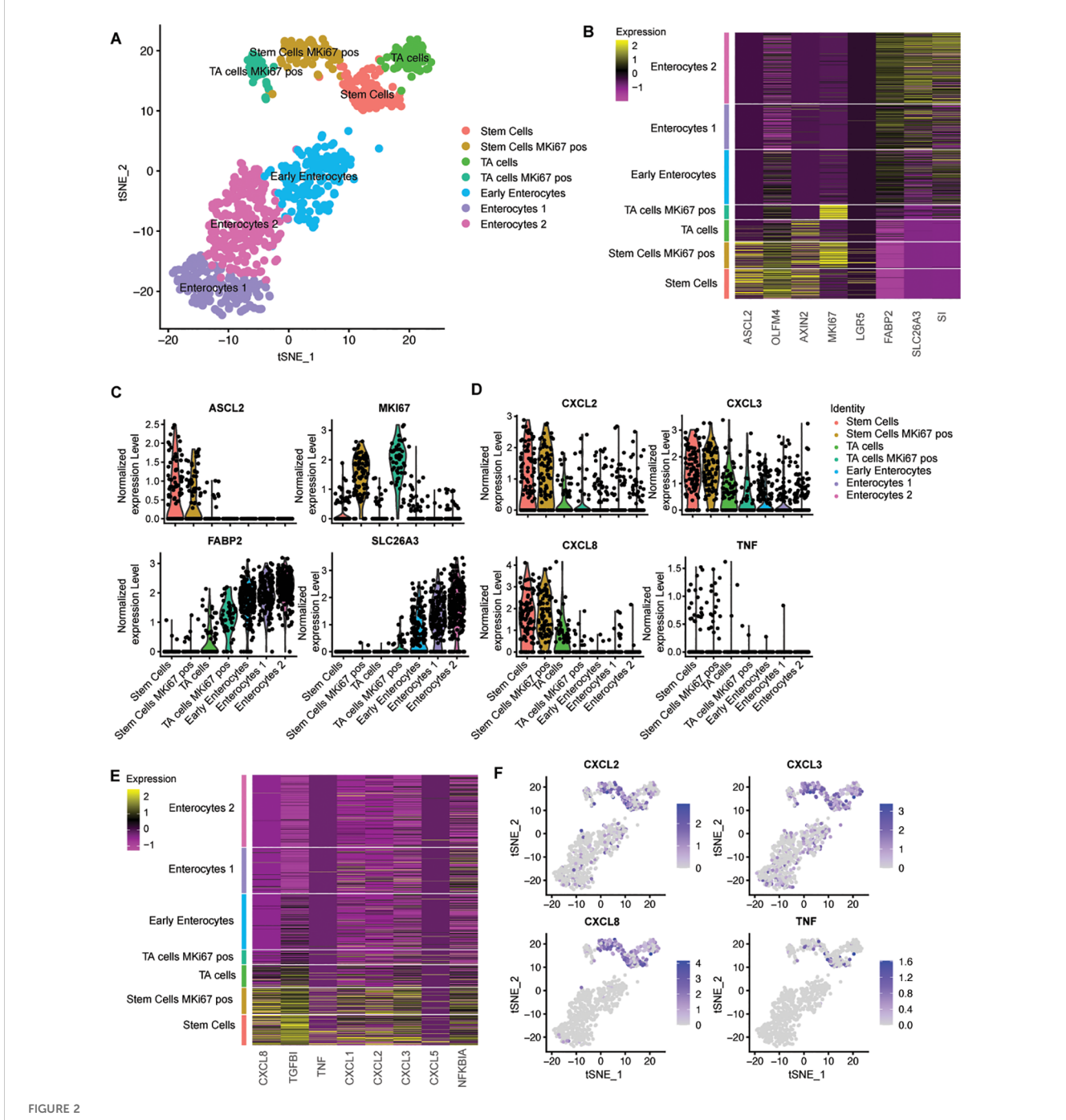
RNA sequencing (scRNAseq) on undifferentiated and differentiated colon organoid cultures exposed to bacterial lysate at the basolateral side. In this analysis, the stem cell and enterocyte conditions were pooled, resulting in a total of 911 cells. The data revealed the presence of seven distinct cell clusters (Figure 2A), which collectively represent the various stages of the three major cell types of IECs that are predominant under these culture conditions. These included stem cells, transit amplifying (TA) cells and enterocytes, which are found in their representative culture condition (Supplementary Figure S3). The stem cells and the transit amplifying cells are composed of two clusters each. The distinctive feature that determines this separation is the cycling activity of cells, which is marked by the expression of MKI67 (Figures 2A-C). Enterocyte-enriched organoids are separated into three clusters. One cluster consisted of enterocytes in the early phase of differentiation, based on the relatively low expression of differentiation markers. The other two clusters contained more differentiated enterocytes (Figures 2A-C).

Subsequently, the expression levels of multiple bacterial response genes were projected onto the identified clusters. Cytokine expression was observed to be higher in the stem cell cluster in comparison to both the transit amplifying cell and the enterocyte clusters. A number of cytokines that are induced upon exposure to bacterial antigens were exclusively expressed within the stem cell clusters (Figures 2D, E). The upregulation of the inflammatory pathway was observed in all stem cells and was independent of *MKI67* expression (Figure 2F), thus excluding cycling activity as a crucial determinant for microbial responsiveness. These analyses confirm that, in comparison to enterocytes, stem cells are the inflammatory responders to microbial molecules among IECs in the large intestine.

To confirm these findings, we also performed scRNAseq on exposed ileum organoids. In a total population of 2027 cells, we identified stem cells, TA cells and enterocytes in three separate clusters (Supplementary Figure S4). Inflammatory responses were confined to the stem and progenitor cells thereby demonstrating that these differences between stem cells and differentiated cells in responsiveness are not specific for the colon but also applies to the small intestine.

### 3.3 The immune response of intestinal stem cell is NF<sub>k</sub>B-mediated

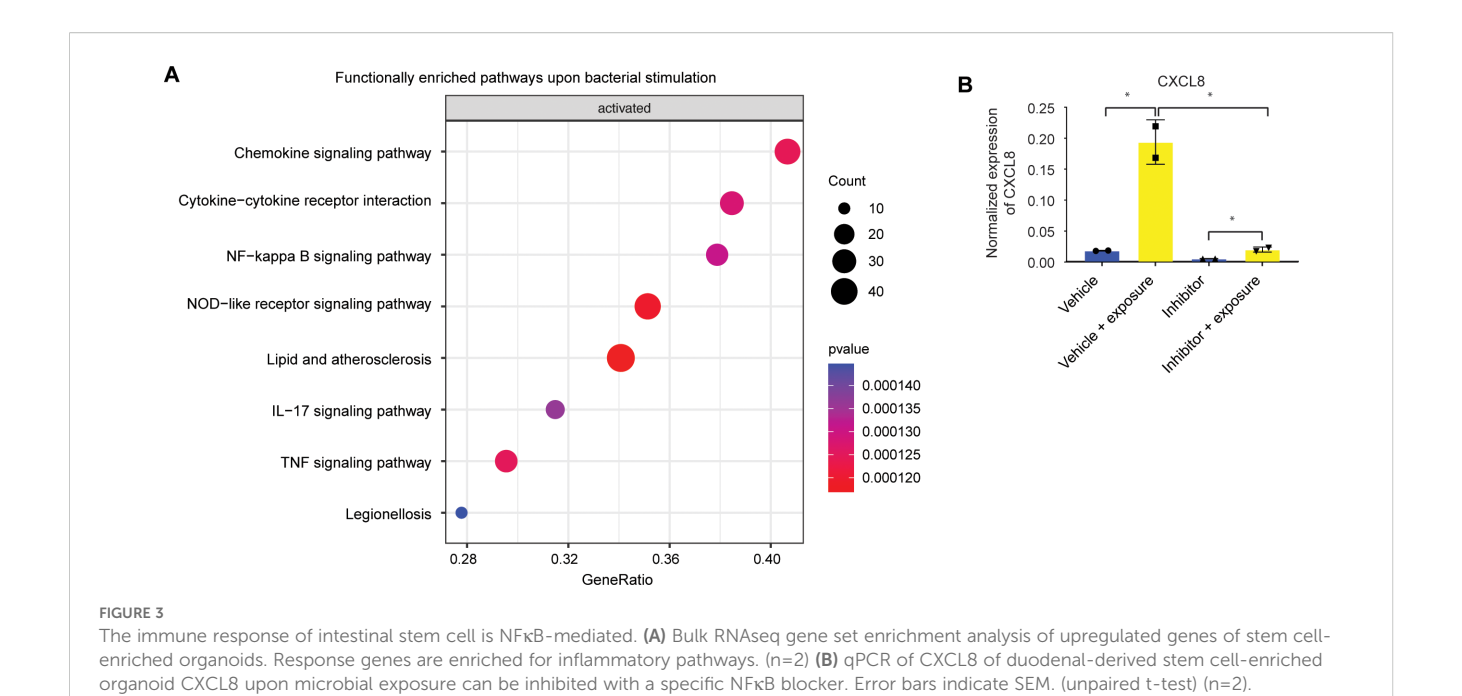
To gain a deeper comprehension of the consequences of bacterial stimulation, we conducted a gene set enrichment



Single cell RNA sequencing shows that intestinal stem cells give a higher inflammatory response compared to enterocytes. (A) tSNE-plot of cell clusters representing different subtypes of IECs. Data were pooled from five days differentiated enterocytes and stem cells colon-derived organoids upon exposure to 6h microbial antigens. (B) Heatmap depicting the expression of stemness and differentiation markers in each identified cell type. (C) Expression of markers that are associated with different states of epithelial differentiation, MKI67, SLC26A3, FABP2 and ASCL2 as determined per cell type. (D) Expression of pro-inflammatory genes per cell type. (E) Heatmap depicting the expression of inflammatory markers for each identified cell type (F) Distribution of expression of CXCL2, CXCL3, CXCL8 and TNFalpha by tSNE-plots. TA = transit amplifying cells; pos = positive.

analysis on bulk RNA transcriptomics, which underwent alterations upon microbial exposure in ISCs. The enriched pathways exhibiting the most pronounced upregulation in undifferentiated organoids were predominantly associated with inflammatory responses (Figure 3A). It is noteworthy that a considerable number of immune response genes are regulated by the NFKB signaling

pathway. However, gene set enrichment analysis did not show any enriched pathways in line with reduced responsiveness of differentiated cells (data not shown). Small molecule inhibition of NF $\kappa$ B during bacterial antigen exposure in undifferentiated organoids indeed resulted in reduced expression of the response gene *CXCL8* (Figure 3B).



### 3.4 Discrepancies in the expression of TLRs and the nuclear translocation of NF $\kappa$ B between stem cells and enterocytes

To elucidate the origin of the discrepancies in responses between stem cells and enterocytes, we conducted a comprehensive examination of the upstream and downstream activity of the NF $\kappa$ B pathway. The activation of NF $\kappa$ B is the result of a complex cascade of activating and inhibitory signals. Pathogen recognition molecules, such as Toll-Like receptors (TLRs), are activated by specific ligands (13). Upon stimulation, these TLRs initiate a signaling cascade that leads to the phosphorylation and nuclear translocation of NF $\kappa$ B, ultimately activating innate immune response genes (50).

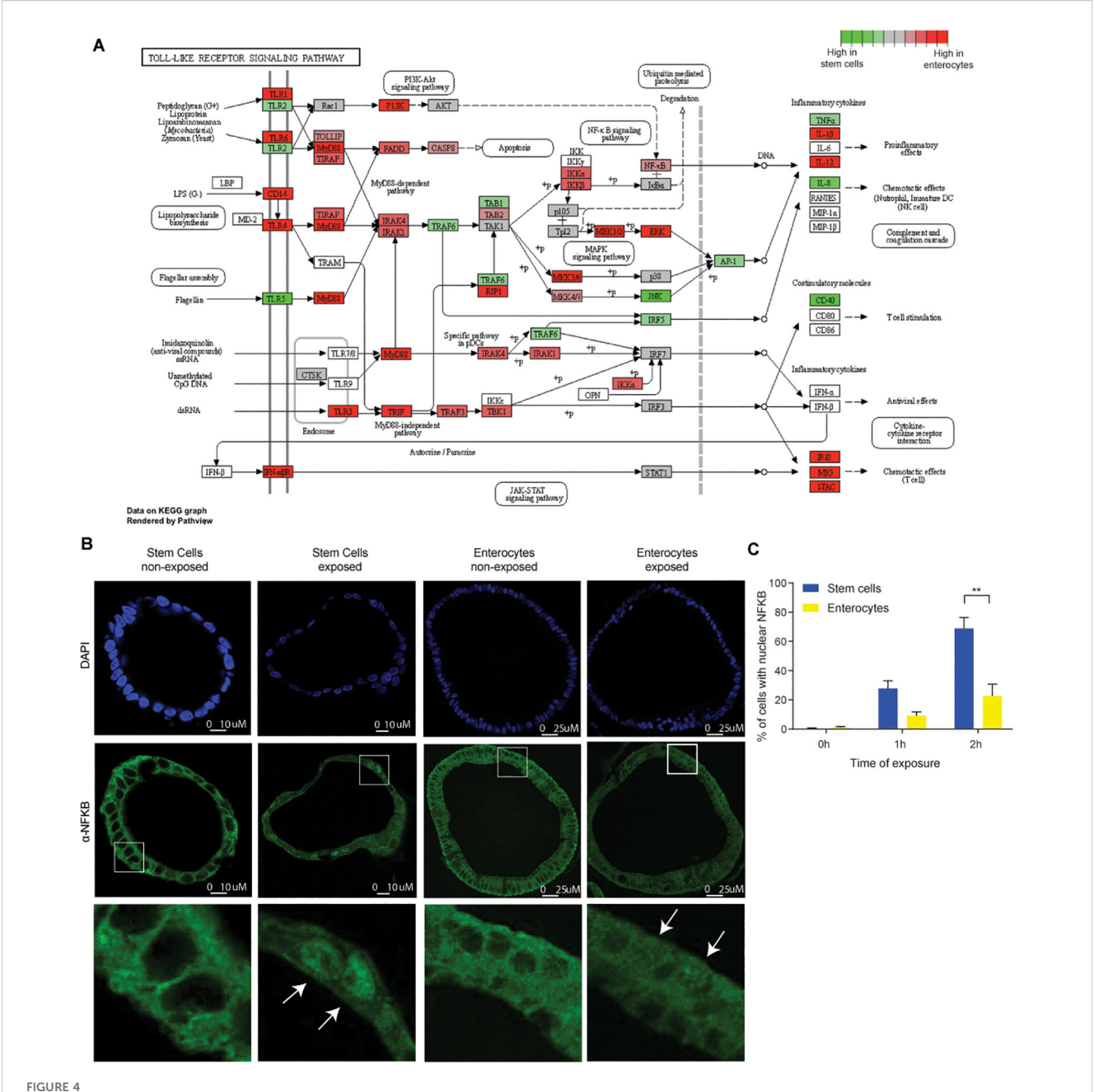
The differential expression of upstream NF¢B components may be responsible for the observed differences in microbial responsiveness between stem cells and enterocytes. Our findings indicated that genes involved in the NF¢B pathway exhibited higher expression levels in enterocyte-enriched organoids than in stem cell-enriched organoids. This suggests that the diminished responsiveness of enterocytes is not attributable to a global downregulation of this pathway (Figure 4A; Supplementary Figure S5).

Notable exceptions to this trend include TLR5 and TLR2, both of which are expressed at higher levels in stem cell-enriched organoids than in enterocyte-enriched organoids. TLR5 is activated by flagellin, while TLR2 is activated by diverse range of microbial ligands (51). Therefore, while the majority of NFκB pathway genes are upregulated during differentiation, the reduced expression of TLR5 and TLR2 in enterocytes may contribute to the diminished response to bacterial lysate. The differential expression of TLRs is consistent with previous findings in mice and pigs (11–13). Interestingly, certain inflammatory mediators, such as IL-1 $\beta$ , IL-12, IP-10, MIG, were more abundant in enterocytes, which could

suggest that some inflammatory pathways are more active in this cell type. It is important to note, however, that there are inherent limitations to estimating pathway activity based on transcript abundance. It is not necessarily the case that there is a direct correlation between RNA transcript quantity and with protein translation (52). An additional limitation is that we do not know through which TLRs the responses are mediated, which would require stimulation with purified TLR agonists instead of whole bacterial lysates. Because of these limitations, it remains difficult to use transcriptomic data to provide an explanation why ISCs are the main responders. Therefore, as direct measure of NFkB pathway activation downstream of TLRs, we also determined the nuclear localization of NFkB. We conducted a comparative analysis of NFκB localization in stem cell- and enterocyte-enriched organoids after 2h of exposure to bacterial lysates. A higher In line with previous observations (53, 54), we observed NF $\kappa$ B translocation to the nucleus upon bacterial antigen exposure (Figures 4B, C). It is noteworthy that nuclear NFKB translocation was highest in ISCs, but also evident in a substantial number of enterocytes, indicating that additional downstream mechanisms may further attenuate the responsiveness of enterocytes to bacterial molecules.

### 3.5 The chromatin in stem cells and enterocytes exhibits equal accessibility and activity of involved promoter sites

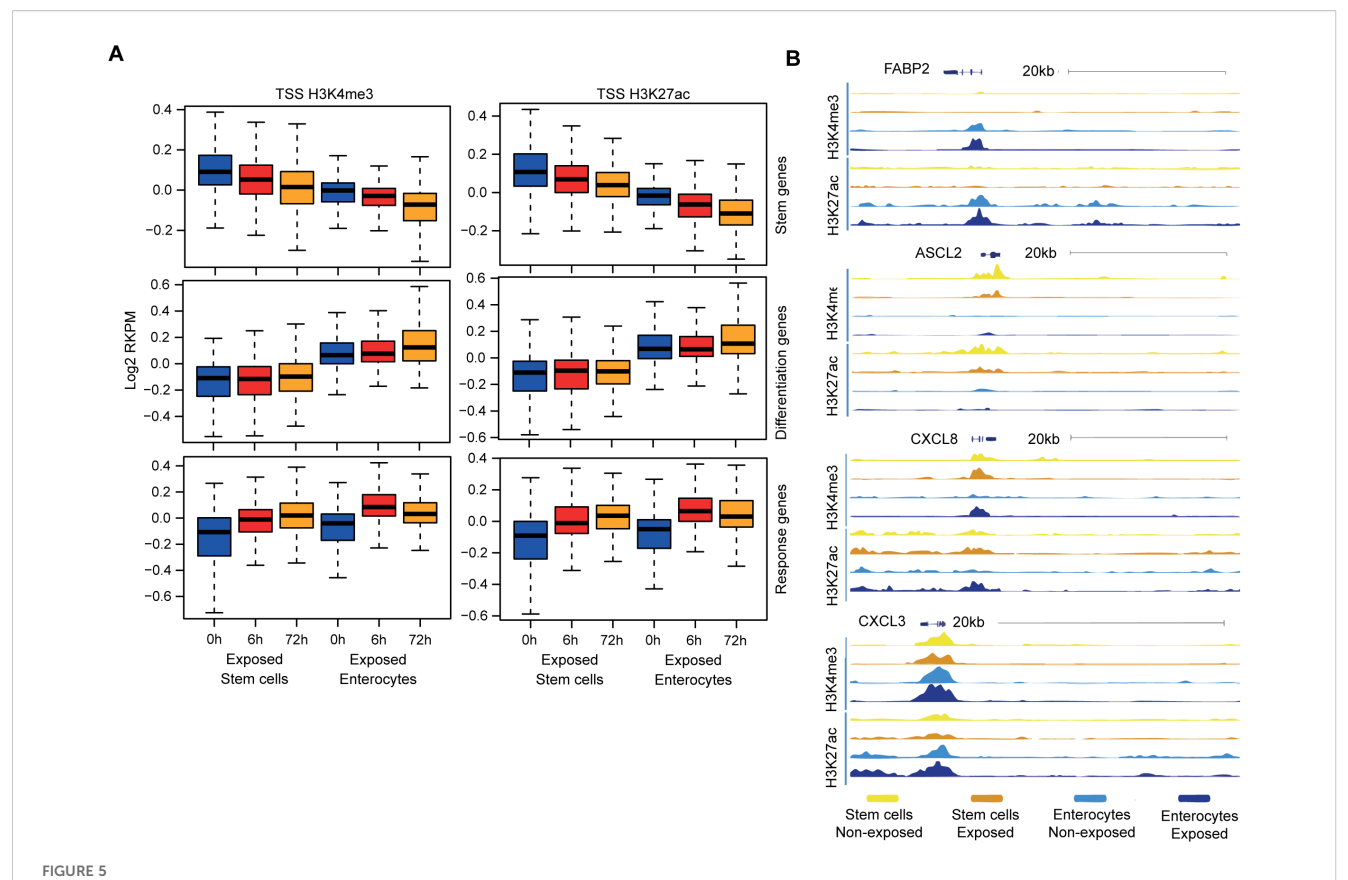
The subsequent analysis aimed to ascertain whether the chromatin accessibility and promoter activity of specific response genes contributes to the diminished microbial responsiveness observed in enterocytes. Chromatin immuno-precipitation (ChIP) was performed on colon organoids for histone modifications H3K4me3 and



Discrepancies in the expression of TLRs and the nuclear translocation of NF $\kappa$ B between stem cells and enterocytes. (A) Bulk RNAseq expression levels of genes involved in Toll Like Receptor signaling pathway in five days differentiated enterocytes-enriched organoids versus stem cell-enriched organoids. (n=2) (B) Immunohistochemistry of NF $\kappa$ B (p65) in stem cell-enriched organoids compared to five days differentiated enterocyte-enriched organoids, shows nuclear translocation of NF $\kappa$ B upon exposure (2h). (n=3) (C) Quantification of nuclear translocation of NF $\kappa$ B. The number of cells with nuclear NF $\kappa$ B is higher in stem cell-enriched organoids compared to enterocyte-enriched organoids (Mann-Whitney). Error bars indicate SEM. (n=3) qPCR: quantitative polymerase chain reaction.

H3K27Ac, which are associated with active gene promoters (55). It is notable that upon exposure to bacterial antigens, both stem cell- and enterocyte-enriched organoids exhibited the presence and induction of active chromatin marks within the promoters of the relevant response genes (Supplementary Table S2), while the promoters of stem cell-associated genes were more active in stem cells and the promoters of differentiation-associated genes were more active in enterocytes (Figure 5A). As example, the promoter region of the differentiation marker *FABP2* is accessible in enterocytes and the promoter region of

the stem cell marker *ASCL2* is accessible in undifferentiated cells. The promoter regions of the response genes *CXCL8* and *CXCL3* become accessible upon stimulation in enterocytes and stem cells (Figure 5B). These findings demonstrate that, even though the upregulation of the mRNAs of response genes is stronger in undifferentiated organoids, enterocyte-enriched organoids retain the ability to activate inflammatory gene promoters upon bacterial antigen exposure. This suggests that the reduced microbial responsiveness of enterocytes is not caused by decreased promoter accessibility.



The chromatin in stem cells and enterocytes exhibits equal accessibility and activity of involved promoter sites. (A) Chromatin immune-precipitation sequencing signal of active histone modifications (H3K4me3, H3K27ac) in the 2kb window around the transcriptional start site of different gene groups – at the baseline and upon exposure to bacterial antigens for 6h and 72h. (values represent median centered and log2 transformed RPKM) (n=2) (B) ChIP tracks at four genomic regions at baseline (-) and upon 6h of exposure to bacterial lysates (+) (n=2).

## 3.6 Evidence that post-transcriptional regulation may play a role in the half-life of genes involved in the epithelial inflammatory response

Prior research has indicated that post-transcriptional regulation may play a role in regulating immune response gene expression by facilitating the rapid degradation of inflammatory transcripts (56, 57). For example, macrophage inflammatory responses are tightly regulated at the post-transcriptional level through AU-rich element (ARE)-mediated mRNA decay (58, 59). This process involves the binding of RNA-binding proteins binding to AREs located in the 3'untranslated region (3'UTR) of mRNAs, which culminates in exonuclease-mediated degradation of the mRNA's poly(A)-tail. This destabilization results in a reduction of the mRNA half-life and the prevention of translation. To ascertain whether AREs are present in IEC transcripts, we conducted an analysis to determine ARE enrichment in specific gene sets. The response genes (i.e. genes that are upregulated upon bacterial antigen exposure in stem cellenriched organoids) exhibited a higher ARE content compared to the stem cell genes (stem genes are genes upregulated in stem cellenriched organoids without exposure) and the differentiation genes (genes upregulated in enterocyte-enriched organoids without exposure) (Supplementary Figure S6A and Supplementary Table S2) (43). This observation is consistent with previous studies that have reported the presence of AREs in approximately 22.4% of human mRNAs, particularly within the 3'UTR of inflammatory genes (43, 60). This finding suggests that inflammatory genes in IECs are susceptible to post-transcriptional regulation (56, 61–63), which may play a role in the immune response of IECs.

The degradation of the poly(A)-tail represents a pivotal step in the pathway of mRNA decay, thus serving as a key determinant of mRNA half-life (64). To explore whether the attenuated inflammatory response in enterocytes could be attributed to increased mRNA decay, we assessed the poly(A)-tail length of transcripts in our organoid models. To measure the poly(A)-tail length, we employed a method involving the addition of guanosine and inosine to the poly(A)-tail, followed by reverse transcription using a 3'UTR-specific primer and a universal reverse primer to generate complementary DNA. Subsequently, the amplified DNA was then analyzed by PCR, and product lengths were determined using agarose gel electrophoresis. The poly(A)-tail length of housekeeping genes (ACTB and GAPDH) and immune response genes (CXCL2, CXCL8, CXCL1, and CCL2) was assessed in stem cell-enriched and enterocyte-enriched organoids exposed to bacterial antigens. The poly(A)-tail length of housekeeping genes remains consistent in both stem cell state and enterocyte state. However, immune response genes exhibit either a similar length

(CXCL1 and CXCL2) or a shorter length in enterocyte-enriched samples (CXCL8 and CCL2) compared to stem cell-enriched samples (Supplementary Figure S6B). These findings suggest that a shorter poly(A)-tail length may contribute to the diminished inflammatory response of enterocytes, potentially due to faster mRNA degradation.

Previous studies have demonstrated that the RNA-binding protein Zinc Finger Protein 36 (also known as TTP and encoded by the gene ZFP36) is capable of binding to AREs and serves as a pivotal mediator in poly(A)-mediated mRNA destabilization, particularly in the context of immune response genes (65). We observe that ZFP36 is higher expressed in enterocytes (Supplementary Figure S6C) compared to stem cells. In contrast, ELAVL1, which encodes a protein (HuR) involved in mRNA stabilization (66), was found to be downregulated in enterocytes compared to stem cells (Supplementary Figure S6D). Earlier studies have demonstrated that the expression of immune response genes and ZFP36 are regulated by NFKB. As such, activated TTP inhibits nuclear translocation of NFKB and downregulates the immune response (67, 68). Our results suggest that HuR and TTP may serve as potential factors that determine the mRNA stability of inflammatory response genes, thereby contributing to the observed differences in responsiveness between the various epithelial cell types. Functional perturbations studies, such as ZFP36 knockdown, are required to confirm this causality.

### 3.7 WNT activation re-establishes inflammatory responses in enterocytes

The WNT/ $\beta$ -catenin pathway plays a pivotal role in the proliferation and maintenance of ISCs in the crypt and as undifferentiated organoids (14, 15) and decreased activity of this pathway induces differentiation (Figure 6A). We observed that undifferentiated organoids with high WNT activity show a stronger response to bacterial antigens than enterocyte organoids with low WNT activity. This may suggest crosstalk between the innate immunity and WNT pathways.

Recent studies in a variety of species and cell types have identified crosstalk between cell identity pathways and immune response pathways (69). To investigate if such crosstalk also exists in IECs, we investigated the effect of modulation of WNT signaling on IEC responsiveness. After 5 days of enterocyte differentiation in the absence of WNT, we stimulated the WNT pathway with WNT3A for a 24h period. While fully differentiated enterocytes do not have the plasticity to de-differentiate to stem cells (28), WNT-stimulation resulted in an increase in *LGR5* expression, confirming robust WNT-pathway activation (Figure 6B). Upon exposure to bacterial lysate in the presence of WNT3A, enterocyte-enriched organoids exhibited an increase in the expression of immune response genes *CXCL8* and *NFKBIA* (Figure 6C). Therefore, the observed increase in response genes suggests a direct involvement of the WNT pathway in the immune response to bacterial antigens.

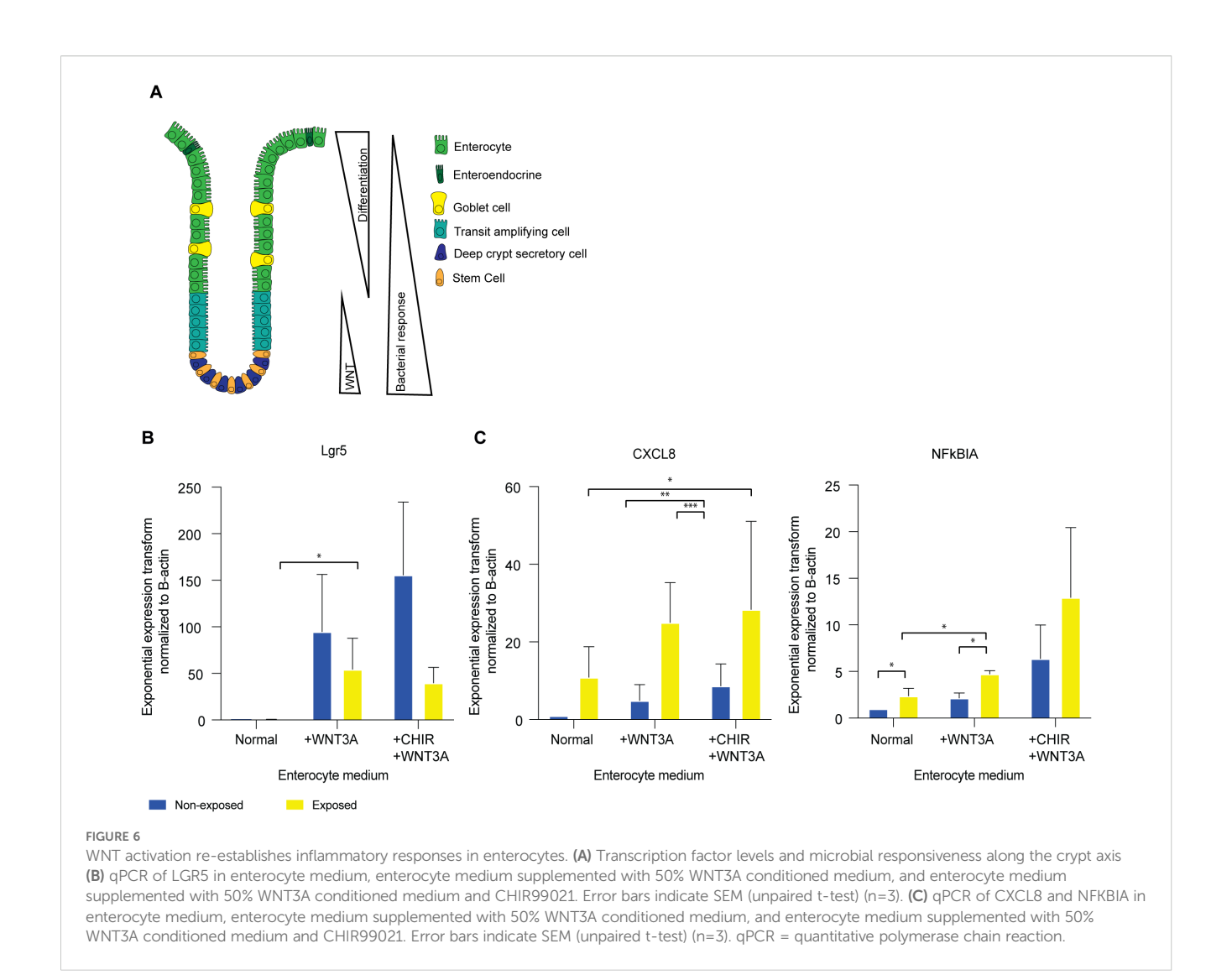
The objective of the subsequent experiment was to ascertain whether the responsiveness of the stem cell-enriched organoids was diminished upon reduced WNT activity. To this aim, WNT3A was removed from the stem cell-enriched condition media to induce differentiation towards enterocytes. Following the withdrawal of WNT3A for a period of 24h, a slight decline in *LGR5* expression was observed (Supplementary Figure S7A). When exposed to bacterial lysate in the absence of WNT3A, *CXCL8* and *NFKBIA* levels are comparable to those observed in stem cell-enriched organoids in the presence of WNT (Supplementary Figure S7B). This suggests that a 24h period of WNT removal may not be sufficient to alter the stem cell state or its associated responsiveness to bacterial antigens.

To further assess whether increased WNT pathway activity modulates the responsiveness of stem cells, we introduced the WNT agonist CHIR99021 into the culture conditions alongside WNT3A for 24h (14). CHIR99021 was administered to stem cell- and enterocyte-enriched organoids. This resulted in an increase in *LGR5* expression (Figure 6B; Supplementary Figure S7A). Upon exposure to bacterial antigen, immune response genes *CXCL8* and *NFKBIA* were upregulated under these conditions (Figure 6C; Supplementary Figure S7B). These results suggest that active WNT signaling enhances the NFκB-mediated immune response to bacterial exposure.

### 4 Discussion

Our findings indicate that the ISCs are the responders to bacterial antigens in the large intestinal epithelium, in contrast to enterocytes. Moreover, our findings indicate that ISCs mainly respond to microbial stimuli when exposed basolaterally. These findings reinforce the mucosal paradigm of the intestinal epithelium, which is designed to avoid the elicitation of inflammatory responses to luminal antigens under homeostatic conditions. Conversely, inflammatory activation is only initiated when microbial antigens penetrate the IEC barrier and reach the basolateral surface of ISCs. The role of the ISCs as epithelial cell responders to microbial stimulation is consistent with previous reports that have identified these cells as having immune functions at the mucosal surfaces of the intestines. T-cell activation has been demonstrated to be contingent upon antigen presentation by ISCs via MHC-II expression (70). Our study demonstrates that, in addition to antigen presentation, ISCs are involved in the mediation of local epithelial immune responses upon exposure to bacterial antigens. We illustrate that the variation in the response between ISCs and enterocytes to bacterial antigens is regulated at multiple levels upstream and downstream of NFκB activation. These findings highlight the intricate regulatory mechanisms that enable ISCs to function as immune mediators in the large intestine.

Lipopolysaccharides (LPS) are a widely utilized compound in the study of bacterial immune responses, as they represent the outer membrane components of gram-negative bacteria (71). However, this approach offers a narrow view of the subject matter, as it does not encompass the full range of bacterial antigens present in more complex systems. In contrast, cecal slurry, prepared from the luminal contents of the colon, contains a more diverse range of bacterial antigens, including bacterial, viral antigens and food particles (72). However, the presence of viral and dietary components in cecal slurry may complicate the analysis of a



bacterial-specific immune response. Here we employed an *E. coli* lysate, which offers a controlled and diverse array of bacterial antigens while circumventing interference from non-bacterial components. This approach ensures a more targeted and reliable evaluation of bacterial immune responses. It would be interesting to extend this approach to other microbial antigens in future studies, to determine the generalizability of our findings.

Our observations indicated differential expression of TLRs and reduced nuclear NFkB translocation in enterocytes, suggesting differential regulation of the processes upstream of NFkB activation. Nevertheless, our results indicate that additional mechanisms may be involved in the diminished microbial responsiveness observed in enterocytes. It was thus established that enterocytes have shortened poly(A)-tails of specific inflammatory transcripts, which is likely to reduce the mRNA stability of these transcripts. It is postulated that mRNA stability in enterocytes is diminished by elevated activity of mRNA degradation pathways. This is corroborated by the observation of high expression of *ZFP36* and low expression of *ELAVL1*, which respectively exert a destabilizing and a stabilizing effect on mRNA. Regulation of the response to bacterial ligands may additionally extend to processes that determine

translational and posttranslational activity. To confirm the hypothesis that posttranscriptional regulation plays a role in the attenuated response of the enterocytes, functional studies are required.

Our findings indicate that in addition to its significant influence on the cell fate of IECs, the activity of the WNT pathway also plays a role in determining epithelial responsiveness. Prior research on other cell types and species has documented crosstalk between WNT/ $\beta$ -catenin signaling and NF $\kappa$ B (73–75). Furthermore,  $\beta$ -catenin has been shown to bind to immune response genes on the DNA, thereby initiating their transcription (76). The results of our study indicate that chromatin accessibility at promoter sites relevant to the inflammatory response is similar between stem cells and differentiated cells. These findings support the hypothesis that specific transcription factors may be directly involved in regulating microbial responsiveness.

The precise molecular mechanism through which WNT activity determines cellular responsiveness remains to be elucidated through further investigation. A potential explanation is through direct interaction between the key players of both pathways,  $\beta$ -catenin and NF $\kappa$ B, as has previously been described (73, 74). Through such interaction,  $\beta$ -catenin could influence the nuclear

translocation of NF $\kappa$ B upon stimulation with bacterial antigen, thereby promoting the NF $\kappa$ B-mediated immune response.

A number of genes are frequently mutated in IBD, and they play a role in the immune pathway. For example, there are mutations identified in the *TLR4*, *IL10R*, and *NFKBIZ* pathways (77–79). The role of post-transcriptional regulation in the setting of inflammatory responses has been previously delineated in the context of immune cells (57). The clinical relevance of these mechanisms is supported by the discovery of a genetic association between *ZFP36* family members (*ZFP36L1*, *ZFP36L2*) and IBD (80–82). Furthermore, some patients with Very Early Onset-IBD have mutations in *TTC37*, which is involved in RNA decay (83, 84). Other gene mutations involved in IBD affect IEC polarization (46, 47, 83). Our data suggest that in cases where the epithelial barrier is compromised or the polarization is disrupted, resulting in exposure of the basolateral side is exposed to the microbiome, an inflammatory response may ensue.

The human organoid cultures lack the complete complexity of cell types present in the native epithelium (85). To profile a heterogeneous population of cell types that constitute the majority of the human intestinal epithelium (86), we combined organoids grown under different culture conditions. In the future, models that include Paneth cells, goblet cells, tuft cells, or deep secretory cells (85) may provide a more comprehensive understanding of the differences in responsiveness among epithelial cells.

The advent of new techniques, such as whole exome sequencing and whole genome sequencing, has the potential to facilitate the discovery of additional genes that may be implicated in IBD. Moreover, the utilization of cutting-edge *in vitro* gut models will facilitate the elucidation of human gut-microbe interactions (30). In light of the findings presented in this study, we anticipate that novel IBD-associated genes will be implicated in the processes upstream and downstream of NF $\kappa$ B and may be involved in pathways ranging from bacteria recognition to the post-transcriptional regulation of response genes, and WNT-signaling.

### Data availability statement

The raw data supporting the conclusions of this article cannot be shared publicly because they contain sensitive patient information and are subject to GDPR and institutional data protection regulations. Relevant data supporting the findings of this study are available from the corresponding author upon reasonable request and following approval by the UMC Utrecht data access committee.

### **Ethics statement**

The studies involving humans were approved by Data collection and research studies were conducted in adherence to the ethical guidelines established by the ethics committees. Human Material Approval for this study was obtained from the Ethics Committees University Medical Center Utrecht (Medisch Ethische Toetsings Commissie (METC) protocol #10/402, titled: Specific Tissue Engineering in Medicine (STEM)) or Boston Children Hospital (protocol #IRB-P00000529, titled: Pediatric Gastrointestinal Disease Biospecimen Repository and Data Registry). The studies were conducted in accordance with the local legislation and institutional requirements. Written informed consent for participation in this study was provided by the participants' legal guardians/next of kin. Written informed consent was obtained from the individual(s), and minor(s)' legal guardian/next of kin, for the publication of any potentially identifiable images or data included in this article.

### **Author contributions**

MdV: Formal Analysis, Writing – original draft, Writing – review & editing, Visualization, Methodology, Investigation. CM: Funding acquisition, Formal Analysis, Writing – review & editing, Investigation, Visualization, Methodology, Writing – original draft. HH: Investigation, Writing – review & editing. AB: Writing – review & editing, Investigation. SJ: Investigation, Writing – review & editing. BK: Investigation, Writing – review & editing. SS: Writing – review & editing, Resources, Funding acquisition. HC: Conceptualization, Writing – review & editing, Funding acquisition. MM: Visualization, Funding acquisition, Writing – review & editing, Methodology, Conceptualization, Supervision, Writing – review & editing, Visualization, Formal Analysis. EN: Supervision, Methodology, Conceptualization, Writing – review & editing, Funding acquisition.

### **Funding**

The author(s) declare financial support was received for the research and/or publication of this article. MdV, CM, EK, MM and EN, were supported by the Leona M. and Harry B. Helmsley Charitable Trust., HC, and SS were supported by NIH (RC2DK122532) Grant. MM was supported by the Career Development grant from MLDS (CDG-15). CM was supported by the Alexandre Suerman stipend of the UMC Utrecht.

### Acknowledgments

We thank Dr. Sabine Middendorp for generating and providing the organoids and Prof. Dr. Sabine Fuchs for maintenance of the organoid biobank.

### Conflict of interest

HC is the head of Pharma Research and Early Development at Roche, Basel, and holds several patents related to organoid

technology. The full disclosure is given at <a href="https://www.uu.nl/staff/ICClevers">https://www.uu.nl/staff/ICClevers</a>.

The remaining authors declare that the research was conducted in the absence of any commercial or financial relationships that could be construed as a potential conflict of interest.

### Generative AI statement

The authors declare that no Generative AI was used in the creation of this manuscript.

Any alternative text (alt text) provided alongside figures in this article has been generated by Frontiers with the support of artificial intelligence and reasonable efforts have been made to ensure accuracy, including review by the authors wherever possible. If you identify any issues, please contact us.

### Publisher's note

All claims expressed in this article are solely those of the authors and do not necessarily represent those of their affiliated organizations, or those of the publisher, the editors and the reviewers. Any product that may be evaluated in this article, or claim that may be made by its manufacturer, is not guaranteed or endorsed by the publisher.

### Supplementary material

The Supplementary Material for this article can be found online at: https://www.frontiersin.org/articles/10.3389/fimmu.2025.1677943/full#supplementary-material

### SUPPLEMENTARY FIGURE 1

(A) Volcano plot of bulk RNAseq of colon enterocytes-enriched organoids 0h versus colon intestinal stem cells-enriched organoids 0h (n=2) (B) Boxplot of intestinal stem cell markers (LGR5, ASCL2) and differentiation markers (VIL1, SLC26A3, and FABP2) in enterocyte- and intestinal stem cell-enriched colon organoids. (n=2).

### References

- 1. Dieterich W, Schink M, Zopf Y. Microbiota in the gastrointestinal tract. *Med Sci (Basel)*. (2018) 6. doi: 10.3390/medsci6040116
- 2. Forbes JD, Van Domselaar G, Bernstein CN. The gut microbiota in immune-mediated inflammatory diseases. *Front Microbiol.* (2016) 7:1081. doi: 10.3389/fmicb.2016.01081
- 3. Damen GM, Hol J, de Ruiter L, Bouquet J, Sinaasappel M, van der Woude J, et al. Chemokine production by buccal epithelium as a distinctive feature of pediatric Crohn disease. *J Pediatr Gastroenterol Nutr.* (2006) 42:142–9. doi: 10.1097/01.mpg.0000189336.70021.8a
- 4. Menckeberg CL, Hol J, Simons-Oosterhuis Y, Raatgeep HR, de Ruiter LF, Lindenbergh-Kortleve DJ, et al. Human buccal epithelium acquires microbial hyporesponsiveness at birth, a role for secretory leukocyte protease inhibitor. *Gut.* (2015) 64:884–93. doi: 10.1136/gutjnl-2013-306149
- 5. Rakoff-Nahoum S, Paglino J, Eslami-Varzaneh F, Edberg S, Medzhitov R. Recognition of commensal microflora by toll-like receptors is required for intestinal homeostasis. *Cell.* (2004) 118:229–41. doi: 10.1016/j.cell.2004.07.002

#### SLIDDI EMENITADY EIGLIDE 2

(A) Expression patterns of inflammatory genes of bulk RNAseq in healthy colon-derived stem cell-enriched organoids (exposed/non-exposed) compared to healthy colon enterocyte-enriched organoids (exposed/non-exposed). (B) qPCR of CXCL8 on colon-derived organoids grown as monolayers upon apical and basolateral exposure to bacterial antigens (unpaired t-test). Error bars indicate SEM (n=4). qPCR = quantitative polymerase chain reaction.

#### SUPPLEMENTARY FIGURE 3

tSNE plot of scRNA-seq data highlighting the stem cell population grown in stem cell medium and the enterocyte population grown in enterocyte medium.

#### SUPPLEMENTARY FIGURE 4

Single cell RNA sequencing shows that ileum stem cells give a higher inflammatory response compared to enterocytes. (A) tSNE-plot of cell clusters representing different subtypes of IECs. Data were pooled from five days differentiated enterocytes and stem cells colon-derived organoids upon exposure to 6h microbial antigens. (B) Heatmap depicting the expression of stemness and differentiation markers in each identified cell type. (C) Expression of markers that are associated with different states of epithelial differentiation, MKI67, SLC26A3, FABP2 and ASCL2 as determined per cell type. (D) Expression of pro-inflammatory genes per cell type. (E) Heatmap depicting the expression of inflammatory markers for each identified cell type (F) Distribution of expression of CXCL2, CXCL3, CXCL8 and TNFalpha by tSNE-plots. TA = transit amplifying cells; pos = positive.

#### SUPPLEMENTARY FIGURE 5

Bulk mRNA expression of Toll-like receptor (TLR) in enterocyte-enriched and stem cell-enriched colon-derived organoids. (A) colon, (B) ileum.

#### SUPPLEMENTARY FIGURE 6

Evidence that post-transcriptional regulation may play a role in the half-life of genes involved in the epithelial inflammatory response. (A) Presence of ARE-elements in 3'UTR of stemness, differentiation and response genes. (Fisher Exact test) (n=2) (B) poly(A) tail length assay 2% agarose gel. Bacterial exposure in stem cells-enriched organoids and enterocyte-enriched organoids for 6h. Marker is 100bp. M=Marker, EN=Enterocytes, SC=Stem Cells. (n=2) (C) Bulk RNA expression of ZFP36 in non-exposed and 6h exposed colon-derived organoids. Error bars indicate SEM. EN=Enterocytes SC=Stem Cells. (n=2) (D) Bulk RNA expression of ELAVL1 in non-exposed and 6h exposed organoids. Error bars indicate SEM. (unpaired t-test) EN=Enterocytes, SC=Stem Cells. (n=2).

### SUPPLEMENTARY FIGURE 7

WNT activation or deactivation and inflammatory responses in intestinal stem cells. (A) qPCR of LGR5 in normal stem cell medium, stem cell medium without WNT3A conditioned medium, and stem cell medium with CHIR99021. Error bars indicate SEM (unpaired t-test) (n=3). (B) qPCR of CXCL8 and NFKBIA in normal stem cell medium, stem cell medium without WNT3A conditioned medium, and stem cell medium with CHIR99021. Error bars indicate SEM (unpaired t-test) (n=3). qPCR = quantitative polymerase chain reaction.

- 6. Rescigno M, Nieuwenhuis EE. The role of altered microbial signaling via mutant NODs in intestinal inflammation. *Curr Opin Gastroenterol.* (2007) 23:21–6. doi: 10.1097/MOG.0b013e32801182b0
- 7. Stumpo DJ, Lai WS, Blackshear PJ. Inflammation: cytokines and RNA-based regulation. Wiley Interdiscip Rev RNA. (2010) 1:60–80. doi: 10.1002/wrna.1
- 8. Pardo-Camacho C, Gonzalez-Castro AM, Rodino-Janeiro BK, Pigrau M, Vicario M. Epithelial immunity: priming defensive responses in the intestinal mucosa. *Am J Physiol Gastrointest Liver Physiol.* (2018) 314:G247–G55. doi: 10.1152/ajpgi.00215.2016
- 9. Pasparakis M. IKK/NF-kappaB signaling in intestinal epithelial cells controls immune homeostasis in the gut. *Mucosal Immunol.* (2008) 1 Suppl 1:S54–7. doi: 10.1038/mi.2008.53
- 10. Netea MG, Schlitzer A, Placek K, Joosten LAB, Schultze JL. Innate and adaptive immune memory: an evolutionary continuum in the host's response to pathogens. *Cell Host Microbe*. (2019) 25:13–26. doi: 10.1016/j.chom.2018.12.006
- 11. Price AE, Shamardani K, Lugo KA, Deguine J, Roberts AW, Lee BL, et al. A map of toll-like receptor expression in the intestinal epithelium reveals distinct spatial, cell

type-specific, and temporal patterns. Immunity.~(2018)~49:560-75e6. doi: 10.1016/j.immuni.2018.07.016

- 12. Gourbeyre P, Berri M, Lippi Y, Meurens F, Vincent-Naulleau S, Laffitte J, et al. Pattern recognition receptors in the gut: analysis of their expression along the intestinal tract and the crypt/villus axis. *Physiol Rep.* (2015) 3(2):e12225. doi: 10.14814/phy2.12225
- 13. Abreu MT. Toll-like receptor signalling in the intestinal epithelium: how bacterial recognition shapes intestinal function. *Nat Rev Immunol.* (2010) 10:131–44. doi: 10.1038/nri2707
- 14. Yin X, Farin HF, van Es JH, Clevers H, Langer R, Karp JM. Niche-independent high-purity cultures of Lgr5+ intestinal stem cells and their progeny. *Nat Methods*. (2014) 11:106–12. doi: 10.1038/nmeth.2737
- 15. Gregorieff A, Pinto D, Begthel H, Destree O, Kielman M, Clevers H. Expression pattern of Wnt signaling components in the adult intestine. *Gastroenterology.* (2005) 129:626–38. doi: 10.1016/j.gastro.2005.06.007
- 16. Jain U, Lai CW, Xiong S, Goodwin VM, Lu Q, Muegge BD, et al. Temporal regulation of the bacterial metabolite deoxycholate during colonic repair is critical for crypt regeneration. *Cell Host Microbe*. (2018) 24:353–63 e5. doi: 10.1016/i.chom.2018.07.019
- 17. Kaiko GE, Ryu SH, Koues OI, Collins PL, Solnica-Krezel L, Pearce EJ, et al. The colonic crypt protects stem cells from microbiota-derived metabolites. *Cell.* (2016) 167:1137. doi: 10.1016/j.cell.2016.10.034
- 18. Schmitt M, Schewe M, Sacchetti A, Feijtel D, van de Geer WS, Teeuwssen M, et al. Paneth cells respond to inflammation and contribute to tissue regeneration by acquiring stem-like features through SCF/c-kit signaling. *Cell Rep.* (2018) 24:2312–28 e7. doi: 10.1016/j.celrep.2018.07.085
- 19. Hoesel B, Schmid JA. The complexity of NF-kappaB signaling in inflammation and cancer. *Mol Cancer*. (2013) 12:86. doi: 10.1186/1476-4598-12-86
- 20. Liu T, Zhang L, Joo D, Sun SC. NF-kappaB signaling in inflammation. Signal Transduct Target Ther. (2017) 2:17023–. doi: 10.1038/sigtrans.2017.23
- 21. Roh TT, Chen Y, Rudolph S, Gee M, Kaplan DL. InVitro models of intestine innate immunity. *Trends Biotechnol.* (2021) 39:274–85. doi: 10.1016/j.tibtech.2020.07.009
- 22. Papp D, Korcsmaros T, Hautefort I. Revolutionizing immune research with organoid-based co-culture and chip systems. *Clin Exp Immunol.* (2024) 218:40–54. doi: 10.1093/cei/uxae004
- 23. Kolawole AO, Wobus CE. Gastrointestinal organoid technology advances studies of enteric virus biology. *PloS Pathog.* (2020) 16:e1008212. doi: 10.1371/journal.ppat.1008212
- 24. Tao L, Reese TA. Making mouse models that reflect human immune responses. Trends Immunol. (2017) 38:181–93. doi: 10.1016/j.it.2016.12.007
- 25. Mestas J, Hughes CC. Of mice and not men: differences between mouse and human immunology. *J Immunol.* (2004) 172:2731–8. doi: 10.4049/jimmunol.172.5.2731
- 26. Langerholc T, Maragkoudakis PA, Wollgast J, Gradisnik L, Cencic A. Novel and established intestinal cell line models An indispensable tool in food science and nutrition. *Trends Food Sci Technol.* (2011) 22:S11–20. doi: 10.1016/j.tifs.2011.03.010
- 27. Middendorp S, Schneeberger K, Wiegerinck CL, Mokry M, Akkerman RD, van Wijngaarden S, et al. Adult stem cells in the small intestine are intrinsically programmed with their location-specific function. *Stem Cells.* (2014) 32:1083–91. doi: 10.1002/stem.1655
- 28. Sato T, Stange DE, Ferrante M, Vries RG, Van Es JH, Van den Brink S, et al. Long-term expansion of epithelial organoids from human colon, adenoma, adenocarcinoma, and Barrett's epithelium. *Gastroenterology.* (2011) 141:1762–72. doi: 10.1053/j.gastro.2011.07.050
- 29. Pleguezuelos-Manzano C, Puschhof J, Rosendahl Huber A, van Hoeck A, Wood HM, Nomburg J, et al. Mutational signature in colorectal cancer caused by genotoxic pks(+) E. coli. *Nature*. (2020) 580:269–73. doi: 10.1038/s41586-020-2080-8
- 30. Puschhof J, Pleguezuelos-Manzano C, Clevers H. Organoids and organs-on-chips: Insights into human gut-microbe interactions. *Cell Host Microbe*. (2021) 29:867–78. doi: 10.1016/j.chom.2021.04.002
- 31. Bornholdt J, Muller CV, Nielsen MJ, Strickertsson J, Rago D, Chen Y, et al. Detecting host responses to microbial stimulation using primary epithelial organoids. *Gut Microbes.* (2023) 15:2281012. doi: 10.1080/19490976.2023.2281012
- 32. Dekkers JF, Wiegerinck CL, de Jonge HR, Bronsveld I, Janssens HM, de Winterde Groot KM, et al. A functional CFTR assay using primary cystic fibrosis intestinal organoids. *Nat Med.* (2013) 19:939–45. doi: 10.1038/nm.3201
- 33. Moon C, VanDussen KL, Miyoshi H, Stappenbeck TS. Development of a primary mouse intestinal epithelial cell monolayer culture system to evaluate factors that modulate IgA transcytosis. *Mucosal Immunol.* (2014) 7:818–28. doi: 10.1038/mi.2013.00
- 34. de Jager W, Prakken BJ, Bijlsma JW, Kuis W, Rijkers GT. Improved multiplex immunoassay performance in human plasma and synovial fluid following removal of interfering heterophilic antibodies. *J Immunol Methods*. (2005) 300:124–35. doi: 10.1016/j.jim.2005.03.009
- 35. Love MI, Huber W, Anders S. Moderated estimation of fold change and dispersion for RNA-seq data with DESeq2. *Genome Biol.* (2014) 15:550. doi: 10.1186/s13059-014-0550-8

- 36. Wu T, Hu E, Xu S, Chen M, Guo P, Dai Z, et al. clusterProfiler 4.0: A universal enrichment tool for interpreting omics data. *Innovation (Camb)*. (2021) 2:100141. doi: 10.1016/j.xinn.2021.100141
- 37. Yu G, Wang LG, Yan GR, He QY. DOSE: an R/Bioconductor package for disease ontology semantic and enrichment analysis. *Bioinformatics*. (2015) 31:608–9. doi: 10.1093/bioinformatics/btu684
- 38. Yu G, Wang LG, Han Y, He QY. clusterProfiler: an R package for comparing biological themes among gene clusters. *OMICS*. (2012) 16:284–7. doi: 10.1089/omi.2011.0118
- 39. Luo W, Friedman MS, Shedden K, Hankenson KD, Woolf PJ. GAGE: generally applicable gene set enrichment for pathway analysis. *BMC Bioinf.* (2009) 10:161. doi: 10.1186/1471-2105-10-161
- 40. Luo W, Brouwer C. Pathview: an R/Bioconductor package for pathway-based data integration and visualization. *Bioinformatics*. (2013) 29:1830–1. doi: 10.1093/bioinformatics/btt285
- 41. Takashima S, Martin ML, Jansen SA, Fu Y, Bos J, Chandra D, et al. T cell-derived interferon-gamma programs stem cell death in immune-mediated intestinal damage. *Sci Immunol.* (2019) 4:eaay8556. doi: 10.1126/sciimmunol.aay8556
- 42. Muraro MJ, Dharmadhikari G, Grun D, Groen N, Dielen T, Jansen E, et al. A single-cell transcriptome atlas of the human pancreas. *Cell Syst.* (2016) 3:385–94 e3. doi: 10.1016/j.cels.2016.09.002
- 43. Bakheet T, Hitti E, Khabar KSA. ARED-Plus: an updated and expanded database of AU-rich element-containing mRNAs and pre-mRNAs. *Nucleic Acids Res.* (2018) 46: D218–D20. doi: 10.1093/nar/gkx975
- 44. Luo L, Lucas RM, Liu L, Stow JL. Signalling, sorting and scaffolding adaptors for Toll-like receptors. *J Cell Sci.* (2019) 133(5):jcs239194. doi: 10.1242/jcs.239194
- 45. Marshall JS, Warrington R, Watson W, Kim HL. An introduction to immunology and immunopathology. *Allergy Asthma Clin Immunol.* (2018) 14:49. doi: 10.1186/s13223-018-0278-1
- 46. Avitzur Y, Guo C, Mastropaolo LA, Bahrami E, Chen H, Zhao Z, et al. Mutations in tetratricopeptide repeat domain 7A result in a severe form of very early onset inflammatory bowel disease. *Gastroenterology*. (2014) 146:1028–39. doi: 10.1053/j.gastro.2014.01.015
- 47. Bigorgne AE, Farin HF, Lemoine R, Mahlaoui N, Lambert N, Gil M, et al. TTC7A mutations disrupt intestinal epithelial apicobasal polarity. *J Clin Invest.* (2014) 124:328–37. doi: 10.1172/JCI71471
- 48. Gassler N, Rohr C, Schneider A, Kartenbeck J, Bach A, Obermuller N, et al. Inflammatory bowel disease is associated with changes of enterocytic junctions.  $Am\ J$   $Physiol\ Gastrointest\ Liver\ Physiol.\ (2001)\ 281:G216-28.\ doi: 10.1152/ajpgi.2001.281.1.G216$
- 49. Vetrano S, Rescigno M, Cera MR, Correale C, Rumio C, Doni A, et al. Unique role of junctional adhesion molecule-a in maintaining mucosal homeostasis in inflammatory bowel disease. *Gastroenterology.* (2008) 135:173–84. doi: 10.1053/j.gastro.2008.04.002
- 50. Christian F, Smith EL, Carmody RJ. The regulation of NF-kappaB subunits by phosphorylation. Cells. (2016) 5. doi: 10.3390/cells5010012
- 51. Simpson ME, Petri WA Jr. TLR2 as a therapeutic target in bacterial infection. Trends Mol Med. (2020) 26:715–7. doi: 10.1016/j.molmed.2020.05.006
- 52. Edfors F, Danielsson F, Hallstrom BM, Kall L, Lundberg E, Ponten F, et al. Genespecific correlation of RNA and protein levels in human cells and tissues. *Mol Syst Biol.* (2016) 12:883. doi: 10.15252/msb.20167144
- 53. Savkovic SD, Koutsouris A, Hecht G. Activation of NF-kappaB in intestinal epithelial cells by enteropathogenic Escherichia coli. *Am J Physiol.* (1997) 273:C1160–7. doi: 10.1152/ajpcell.1997.273.4.C1160
- 54. Cario E, Rosenberg IM, Brandwein SL, Beck PL, Reinecker HC, Podolsky DK. Lipopolysaccharide activates distinct signaling pathways in intestinal epithelial cell lines expressing Toll-like receptors. *J Immunol.* (2000) 164:966–72. doi: 10.4049/immunol.164.2.966
- 55. Heintzman ND, Stuart RK, Hon G, Fu Y, Ching CW, Hawkins RD, et al. Distinct and predictive chromatin signatures of transcriptional promoters and enhancers in the human genome. *Nat Genet*. (2007) 39:311–8. doi: 10.1038/ng1966
- 56. Chen CY, Shyu AB. AU-rich elements: characterization and importance in mRNA degradation. *Trends Biochem Sci.* (1995) 20:465–70. doi: 10.1016/S0968-0004 (00)89102-1
- 57. Carpenter S, Ricci EP, Mercier BC, Moore MJ, Fitzgerald KA. Post-transcriptional regulation of gene expression in innate immunity. *Nat Rev Immunol.* (2014) 14:361–76. doi: 10.1038/nri3682
- 58. Carballo E, Lai WS, Blackshear PJ. Feedback inhibition of macrophage tumor necrosis factor-alpha production by tristetraprolin. *Science*. (1998) 281:1001–5. doi: 10.1126/science.281.5379.1001
- 59. Stoecklin G, Anderson P. Posttranscriptional mechanisms regulating the inflammatory response. *Adv Immunol.* (2006) 89:1–37. doi: 10.1016/S0065-2776(05) 89001-7
- 60. Bakheet T, Khabar KSA, Hitti EG. Differential upregulation of AU-rich element-containing mRNAs in COVID-19. *Hum Genomics*. (2022) 16:59. doi: 10.1186/s40246-022-00433-9

- 61. Chen CY, Xu N, Shyu AB. mRNA decay mediated by two distinct AU-rich elements from c-fos and granulocyte-macrophage colony-stimulating factor transcripts: different deadenylation kinetics and uncoupling from translation. *Mol Cell Biol.* (1995) 15:5777–88. doi: 10.1128/MCB.15.10.5777
- 62. Otsuka H, Fukao A, Funakami Y, Duncan KE, Fujiwara T. Emerging evidence of translational control by AU-rich element-binding proteins. *Front Genet.* (2019) 10:332. doi: 10.3389/fgene.2019.00332
- 63. Vlasova-St Louis I, Bohjanen PR. Post-transcriptional regulation of cytokine signaling by AU-rich and GU-rich elements. *J Interferon Cytokine Res.* (2014) 34:233–41. doi: 10.1089/jir.2013.0108
- 64. Passmore LA, Coller J. Roles of mRNA poly(A) tails in regulation of eukaryotic gene expression. Nat Rev Mol Cell Biol. (2022) 23:93–106. doi: 10.1038/s41580-021-00417-y
- 65. Lykke-Andersen J, Wagner E. Recruitment and activation of mRNA decay enzymes by two ARE-mediated decay activation domains in the proteins TTP and BRF-1. *Gene Dev.* (2005) 19:351–61. doi: 10.1101/gad.1282305
- 66. Dean JL, Wait R, Mahtani KR, Sully G, Clark AR, Saklatvala J. The 3' untranslated region of tumor necrosis factor alpha mRNA is a target of the mRNA-stabilizing factor HuR. *Mol Cell Biol.* (2001) 21:721–30. doi: 10.1128/MCB.21.3.721-730.2001
- 67. Chen YL, Jiang YW, Su YL, Lee SC, Chang MS, Chang CJ. Transcriptional regulation of tristetraprolin by NF-kappaB signaling in LPS-stimulated macrophages. *Mol Biol Rep.* (2013) 40:2867–77. doi: 10.1007/s11033-012-2302-8
- 68. Schichl YM, Resch U, Hofer-Warbinek R, de Martin R. Tristetraprolin impairs NF-kappaB/p65 nuclear translocation. *J Biol Chem.* (2009) 284:29571–81. doi: 10.1074/jbc.M109.031237
- 69. de Vries MH, Kuijk EW, Nieuwenhuis EES. Innate immunity of the gut epithelium: Blowing in the WNT? *Mucosal Immunol.* (2025). doi: 10.1016/j.mucimm.2025.06.004
- 70. Biton M, Haber AL, Rogel N, Burgin G, Beyaz S, Schnell A, et al. T helper cell cytokines modulate intestinal stem cell renewal and differentiation. *Cell.* (2018) 175:1307–20 e22. doi: 10.1016/j.cell.2018.10.008
- 71. Farhana A, Khan YS. Biochemistry, lipopolysaccharide. Treasure Island (FL: StatPearls (2024).
- 72. Rincon JC, Efron PA, Moldawer LL, Larson SD. Cecal slurry injection in neonatal and adult mice. *Methods Mol Biol.* (2021) 2321:27–41. doi: 10.1007/978-1-0716-1488-4\_4
- 73. Ma B, Hottiger MO. Crosstalk between wnt/beta-catenin and NF-kappaB signaling pathway during inflammation. *Front Immunol.* (2016) 7:378. doi: 10.3389/fimmu.2016.00378
- 74. Deng J, Miller SA, Wang HY, Xia W, Wen Y, Zhou BP, et al. beta-catenin interacts with and inhibits NF-kappa B in human colon and breast cancer. *Cancer Cell.* (2002) 2:323–34. doi: 10.1016/S1535-6108(02)00154-X

- 75. Du Q, Geller DA. Cross-regulation between wnt and NF-kappaB signaling pathways. For Immunopathol Dis Therap. (2010) 1:155–81. doi: 10.1615/ForumImmunDisTher.v1.i3
- 76. Schuijers J, Mokry M, Hatzis P, Cuppen E, Clevers H. Wnt-induced transcriptional activation is exclusively mediated by TCF/LEF. *EMBO J.* (2014) 33:146–56. doi: 10.1002/embj.201385358
- 77. Kakiuchi N, Yoshida K, Uchino M, Kihara T, Akaki K, Inoue Y, et al. Frequent mutations that converge on the NFKBIZ pathway in ulcerative colitis. *Nature*. (2020) 577:260–5. doi: 10.1038/s41586-019-1856-1
- 78. Feki S, Bouzid D, Abida O, Chtourou L, Elloumi N, Toumi A, et al. Genetic association and phenotypic correlation of TLR4 but not NOD2 variants with Tunisian inflammatory bowel disease. *J Dig Dis.* (2017) 18:625–33. doi: 10.1111/1751-2980.12552
- 79. Kotlarz D, Beier R, Murugan D, Diestelhorst J, Jensen O, Boztug K, et al. Loss of interleukin-10 signaling and infantile inflammatory bowel disease: implications for diagnosis and therapy. *Gastroenterology*. (2012) 143:347–55. doi: 10.1053/j.gastro.2012.04.045
- 80. Jostins L, Ripke S, Weersma RK, Duerr RH, McGovern DP, Hui KY, et al. Host-microbe interactions have shaped the genetic architecture of inflammatory bowel disease. *Nature*. (2012) 491:119–24. doi: 10.1038/nature11582
- 81. Meddens CA, Harakalova M, van den Dungen NA, Foroughi Asl H, Hijma HJ, Cuppen EP, et al. Systematic analysis of chromatin interactions at disease associated loci links novel candidate genes to inflammatory bowel disease. *Genome Biol.* (2016) 17:247. doi: 10.1186/s13059-016-1100-3
- 82. Nanki K, Fujii M, Shimokawa M, Matano M, Nishikori S, Date S, et al. Somatic inflammatory gene mutations in human ulcerative colitis epithelium. *Nature*. (2020) 577:254–9. doi: 10.1038/s41586-019-1844-5
- 83. Rahmani F, Rayzan E, Rahmani MR, Shahkarami S, Zoghi S, Rezaei A, et al. Clinical and mutation description of the first Iranian cohort of infantile inflammatory bowel disease: the Iranian primary immunodeficiency registry (IPIDR). *Immunol Invest.* (2021) 50:445–59. doi: 10.1080/08820139.2020.1776725
- 84. Kammermeier J, Drury S, James CT, Dziubak R, Ocaka L, Elawad M, et al. Targeted gene panel sequencing in children with very early onset inflammatory bowel disease–evaluation and prospective analysis. *J Med Genet*. (2014) 51:748–55. doi: 10.1136/jmedgenet-2014-102624
- 85. Fujii M, Matano M, Toshimitsu K, Takano A, Mikami Y, Nishikori S, et al. Human intestinal organoids maintain self-renewal capacity and cellular diversity in niche-inspired culture condition. *Cell Stem Cell*. (2018) 23:787–93 e6. doi: 10.1016/j.stem.2018.11.016
- 86. Barker N, van de Wetering M, Clevers H. The intestinal stem cell. *Genes Dev.* (2008) 22:1856–64. doi: 10.1101/gad.1674008